Chemical Engineering Journal 156 (2010) 177–183

Contents lists available at ScienceDirect

Chemical Engineering Journal

journal homepage: www.elsevier.com/locate/cej

New approach for simultaneous enhancement of anticorrosive and mechanical properties of coatings: Application of water repellent nano $CaCO_3$–PANI emulsion nanocomposite in alkyd resin

B.A. Bhanvase, S.H. Sonawane*

Department of Chemical Engineering, Vishwakarma Institute of Technology, 666, Upper Indira Nagar, Pune 411 037, India

ARTICLE INFO

Article history:
Received 28 February 2009
Received in revised form
28 September 2009
Accepted 6 October 2009

Keywords:
Functional nano $CaCO_3$
Nanocomposites
Anticorrosive alkyd coatings
Mechanical properties

ABSTRACT

New alkyd coatings were prepared by addition of water-based polyaniline–4% $CaCO_3$ (PAC) nanocomposites into alkyd resin. Pure polyaniline (PANI) and PAC were synthesized using ultrasound assisted emulsion polymerization and added to alkyd resin to form nanocomposite coating. Nano $CaCO_3$ was added in different percentage ranging from 0% to 8% of monomer during the synthesis of polyaniline. XRD and TEM reveals that water repellent nano $CaCO_3$ is thoroughly dispersed in PANI matrix. The effect of PANI and PAC nanocomposite on mechanical and anticorrosion performance of alkyd coating was evaluated. An electrochemical measurement (Tafel Plots) shows that corrosion current I_{corr} was decreased from 0.89 to 0.03 $\mu A/cm^2$, when PAC nanocomposite was added to neat coatings. Positive shift of $E_{corr.}$ also indicates that PAC nanocomposite acts as an anticorrosive additive to alkyd coating. Presence of water repellant nano $CaCO_3$ in PAC nanocomposite has exhibited dual effect, such as improvement in mechanical and anticorrosion properties. The experimental results have shown superiority of PAC nanocomposite over PANI when PAC nanocomposite added to alkyd coatings.

1. Introduction

Protection of steel structure from corrosion by organic coatings is a well known practice. These coated systems use commercial micro size pigments to improve their corrosion resistance and mechanical properties. Commercially available inorganic pigments however, are associated with number of drawbacks. e.g., problems like poor adhesion, reduced coating flexibility, loss of impact resistance, loss of optical transparency, inferior abrasion and scratch resistance [1–3]. The loading level required for conventional pigments is quite high, which is dictated by the amount of material necessary to satisfy their function [4]. With the quest for new developed coating systems with better performance, use of nanomaterials in coating is the most recent practice. The improvement in the properties of the nano coatings is attributed to their small size of pigments and fillers [5]. Nanomaterials mostly used in coating system, normally are SiO_2 [3], TiO_2 [6], ZnO [7], Al_2O_3 [8], Fe_2O_3 [9] and also some metals like nano-aluminum [10], nano-titanium [11], etc. are also being used for modifying the organic coatings. Alkyd resin is generally used as vehicle in number of surface coatings formulations. Generally water-based synthesized polyaniline is being added during coating formation along with alkyd resin so as to enhance the anticorrosive property of the surface coating [12–14]. Jaroslav et al. [12] synthesized particles of zinc ferrite, $ZnO{\cdot}Fe_2O_3$, and were coated with polyaniline phosphate during the in situ polymerization of aniline in an aqueous solution of phosphoric acid. They found that the ferrite alone can act as an oxidant for aniline. It is known that the use of water repellent nano $CaCO_3$ coated with MA will act as barrier to water and hence can enhance the corrosion inhibition mechanism, which is not studied in detail earlier. Further, use of actual anticorrosive pigments such as Fe_2O_3 can be minimized as they are costlier as compared to synthesized innovative nanoparticles. It is also possible to improve both mechanical and anticorrosive properties.

Although a variety of conducting polymers have been synthesized and investigated, polyaniline is known for good conductivity and environmental stability [15]. Polyaniline and its derivatives have been extensively used as anticorrosive coatings on metals [16–20]. However, a pure coating of polyaniline and its derivatives suffers from low mechanical properties and adhesion to the substrate [21,22]. It is reported that, for simultaneous improvement in mechanical, adhesion and anticorrosive properties PANI composite could be prepared along with inorganic additives/filler [23–26].

Calcium carbonate is common filler that can be used in a variety of sizes and shape. It is reported that surface treatment of calcium carbonate play important role for miscibility of nano $CaCO_3$ in composite coatings [27,28].

* Corresponding author. Tel.: +91 20 24202224; fax: +91 20 24280926.
E-mail address: shirishsonawane@rediffmail.com (S.H. Sonawane).

1385-8947/$ – see front matter © 2009 Elsevier B.V. All rights reserved.
doi:10.1016/j.cej.2009.10.013

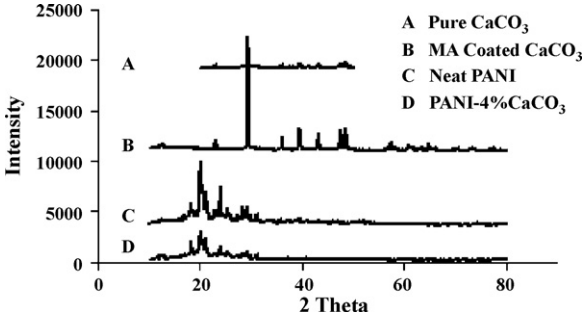

Fig. 1. XRD pattern of (A) pure $CaCO_3$ (B) MA coated $CaCO_3$ (C) neat PANI and (D) PANI-4% $CaCO_3$ nanocomposite.

The objective of the present study is in threefold; (1) Study the feasibility of application of PAC nanocomposite in alkyd resin as anticorrosive composite, (2) To assess simultaneous improvement in mechanical and anticorrosive properties of coating, and (3) Investigate and explain the plausible mechanism of anticorrosive behavior of the coating. In the present work, PAC nanocomposite was synthesized using emulsion polymerization technique. PANI and PAC nanocomposite is dispersed in solvent based alkyd resin in varying percentage. The effect of addition of PANI and PAC nanocomposite on the anticorrosive and mechanical properties of the alkyd resin is explained on the basis of the structure, characterization and morphology analysis.

2. Experimental

2.1. Materials

The monomer aniline (analytical grade, M/s Fluka) was distilled two times prior to use. Ammonium persulphate (APS, $(NH_4)_2S_2O_8$), sodium lauryl sulphate (SLS) were of analytical grade from M/s CDH. Xylene and other chemicals were of analytical grade and were procured from M/s Thomas Baker. Alkyd resin (Soya Alkyd Semidrying type) of Industrial grade was purchased from M/s Mahuli Paints, Pune, India.

2.2. Semi-batch emulsion polymerization of PANI and PAC nanocomposite

Synthesis of functional MA coated $CaCO_3$ was carried out by using innovative method, i.e., by passing CO_2 gas through calcium hydroxide slurry and myristic acid was introduced along with methanol (methanol: MA = 4:1 wt basis). The detailed procedure of sonochemical carbonization is reported by Sonawane et al. [29,30]. Following steps were involved while preparing PANI. In a separate beaker, surfactant solution was prepared by adding of 3 g SLS in 50 ml water. The initiator solution was prepared by adding 7.33 g of APS in 30 ml of deionized water and then was transferred to a semi-batch reactor. In the first instance, 1 g of aniline was added to the reactor and remaining 8 g was added dropwise. This addition process was completed within a span of 70 min. Reaction temperature was maintained at 4 °C (±0.5) throughout the experimental investigation. All the experiments were carried out in ultrasonic bath (Sonics and Materials, 20 kHz, 600 W) so as to enhance the reaction rate and micro-mixing of reaction mass. After a time lapse of 20 min a dark green suspension was observed, which goes to confirm the formation of PANI. The reaction was continued for a further period of 90 min and then the resulting polymerized colloidal dispersion was kept undisturbed for 2 h. The precipitate was separated from the solution by filtration. The recovered precipitate was then washed thoroughly with deionized water and subsequently dried in a oven for 48 h at 60 °C (±1).

A PAC nanocomposite was prepared in the similar manner as mentioned above. Nano $CaCO_3$ percentage was varied from 2% to 8% of monomer quantity and was added to the reactor along with SLS. As reaction progressed, the formation of a thick orange solution was initially observed (the color of PAC nanocomposite was found different than PANI), which then transformed into a dark green suspension. In both the synthesis the conversion of monomer is more than 98%, which was measured gravimetrically.

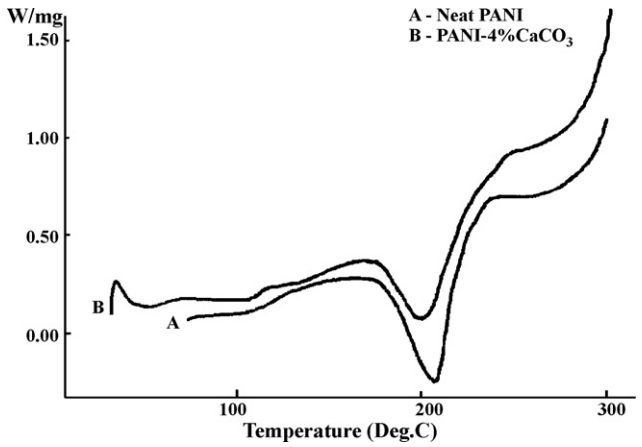

Fig. 2. DSC thermograms (A) neat PANI, (B) PANI + 4% $CaCO_3$.

2.3. Preparation of PANI and PAC/alkyd coatings

PANI-alkyd coatings were prepared using pigment muller and by dispersing 1.0, to 5.0 wt.% PANI in alkyd resin. The prepared coating was thoroughly mixed with xylene solution so that application of coating by using brush will become quite easy. Similarly, the PAC/alkyd was prepared by dispersing 1.0, to 5.0 wt.% of PAC nanocomposite in alkyd resin. PAC/alkyd coatings were applied by using brush on steel panels having dimensions $90 \times 57 \times 1$ mm.

2.4. Property testing and characterization of PANI, PAC nanocomposite and coatings

XRD diffraction patterns of PANI and PAC nanocomposite were recorded by using powder X-ray diffractometer (Philips PW 1800). The Cu-Kα radiation (LFF tube 35 kV, 50 mA) was utilized for the analytical purpose. Transmission electron microscopy (TEM) was performed on Technai G20- stwin working at 200 kV. The thickness of the coating film on mild steel (MS) plate was maintained close to 50 μm. Mechanical and physical property testing for cross-cut adhesion, impact resistance test and gloss at 45° were evaluated as per ASTM standards. Corrosion tests were conducted in acid, alkali,

Table 1
Physico-mechanical characteristics of PANI/$CaCO_3$/alkyd coatings.

Resin	Cross-cut adhesion ASTM D 3359-87	Gloss (at 45°)	Impact resistance (kg/cm^2) ASTM D2794
Alkyd	1 mm Fail	25	60
1.0% PANI/alkyd	1 mm Pass	45	70
1.5% PANI/alkyd	1 mm Pass	30	71
2.0% PANI/alkyd	1 mm Pass	35	73
2.5% PANI/alkyd	1 mm Pass	47	74
5.0% PANI/alkyd	1 mm Pass	33	78
1.0% PAC/alkyd	1 mm Pass	56	92
1.5% PAC/alkyd	1 mm Pass	62	95
2.0% PAC/alkyd	1 mm Pass	55	97
2.5% PAC/alkyd	1 mm Pass	56	98
5.0% PAC/alkyd	1 mm Pass	45	102

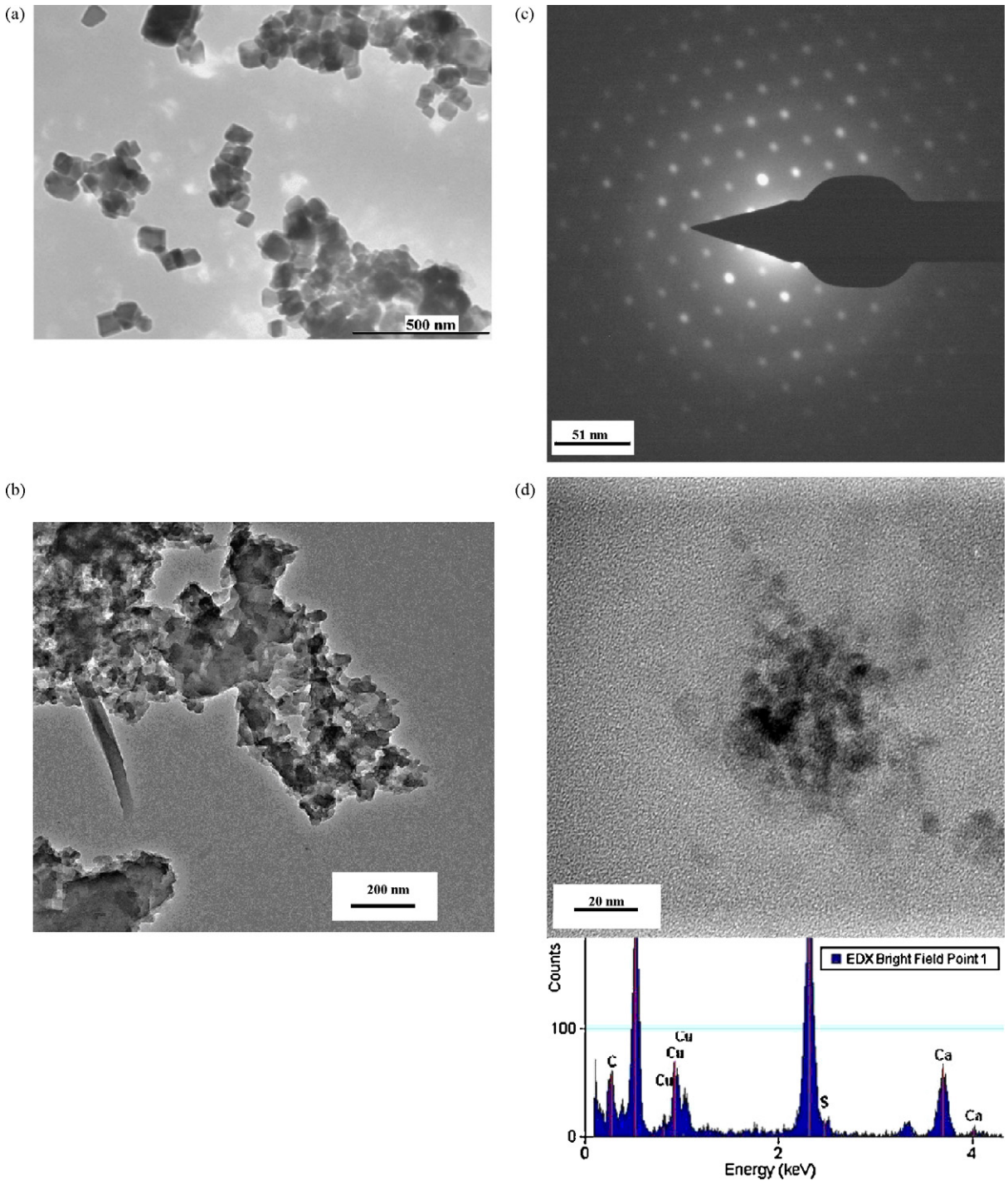

Fig. 3. Transmission electron microscopic images of (a) MA coated nano $CaCO_3$; (b) pure PANI; (c) pure PANI (for single particle); (d) EDAX Analysis and Transmission electron microscopic images of PANI/$CaCO_3$ nanocomposite.

and salt solution (HCl, NaOH, NaCl: 5 wt.% each) by placing the steel strips in porcelain dishes having 15 cm diameter and coated samples were immersed in test media till deterioration occurred and cracks were developed. Each sample was under media for nearly 200 h. The protective behavior of the coatings against the dissolution of MS was evaluated by calculating the corrosion rate (Vc) for each one of the samples [31,32] by using the expression (1):

$$Vc = \frac{\Delta g}{(A\ t\ d)} \quad (1)$$

where Δg is the weight loss in grams for each sample, A is the exposed area of the sample in cm^2, t is the time of exposure in years, and d is the density of the metallic species in g/cm^3. The weight loss was measured after carefully washing the samples with distilled water till the deposited corrosion product was removed, and finally, moisture was removed from the samples by drying at 60 °C (±1) in a oven.

Tafel plot ($\log|I|$ vs. E) was carried out in 5% NaCl solution as electrolyte. All measurements were performed on computerized electrochemical analyzer (supplied by Autolab Instruments, Netherland). Three different MS plates coated with neat alkyd resin,

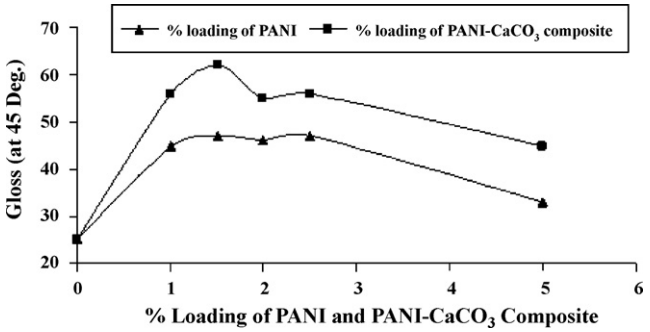

Fig. 4. Variation of gloss with loading of PANI and PANI/$CaCO_3$ in alkyd.

5% PANI dispersed in alkyd resin and 5% PAC nanocomposite dispersed in alkyd resin respectively were used as working electrode, while Pt and silver/silver chloride were used as counter and reference electrode respectively. The area of 1 cm^2 was used for testing. The electrochemical window is −2 V to +1 V with 50 mV/s scanning rate. Electrochemical measurements were carried out at room temperature (25 °C).

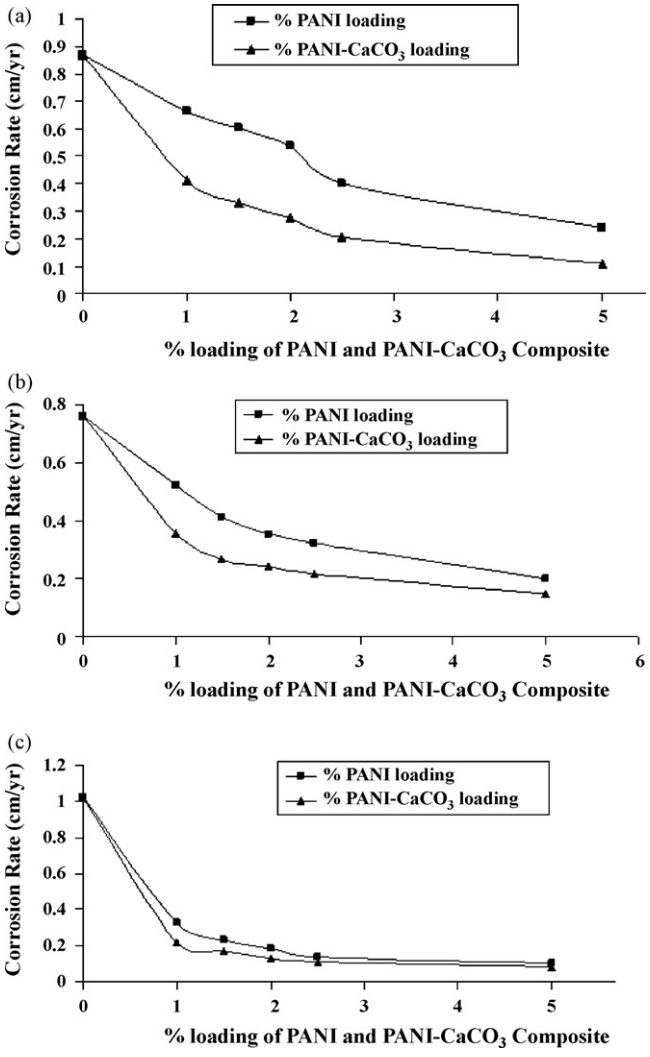

Fig. 5. Corrosion-protective efficiency of PANI/alkyd and PANI/$CaCO_3$/alkyd coatings in (a) 5% HCl; (b) 5% NaCl; (c) 5% NaOH.

3. Results and discussion

3.1. Size, dispersion properties and nature of PANI and PAC nanocomposite

X-ray diffraction pattern of pure $CaCO_3$ and MA coated $CaCO_3$ is shown in Fig. 1A and B. It is found that due to presence of myristic acid (surfactant), the particle size is reduced from 56 (pure nano $CaCO_3$) to 20 nm. It is also found that no change in phase was observed due to addition of myristic acid. As reported in our previous work [29,30] due to presence of surfactant, drop in induction time occurs; hence reduction in particle size is obtained, while no alteration in phase (calcite) is observed. X-ray diffraction pattern of neat PANI (0 wt.% of $CaCO_3$) is shown in Fig. 1C. Diffraction pattern at different 2θ values i.e. $2\theta = 18.3°$, 20.1°, 21.1°, 24°, 28.4°, 29.2°, highlights the characteristic peak of PANI [33,34]. The XRD pattern of PAC nanocomposite with 4 wt.% of $CaCO_3$ in PANI is shown in Fig. 1D. The diffraction pattern of PAC nanocomposite shows a sharp peak at $2\theta = 12.3°$, 18.2°, 20.1°, 21.1°, 24°. It is found that, there is a slight shift of PANI peak in these nanocomposite. The peaks of PAC nanocomposite exhibit a semi-crystalline nature.

Fig. 2 shows the DSC thermogram of neat PANI and PAC nanocomposite. It is found that the addition of nanoparticles in the nanocomposite affects the thermal behavior of PAC nanocomposite. A smooth thermogram is seen along with the single peak for neat PANI, while for PAC nanocomposite the thermogram shows two exothermic peaks. This may be attributed to the fact that interaction of nanoparticle surface with polymer functionalities, resulting in the initiation of cross-linking reaction at lower temperature. The value of ΔH (heat of reaction) for neat PANI is higher as compared to PAC nanocomposite (−123.21 J/g for PANI and −89.20 J/g for PAC nanocomposite). The curing temperature is also found to be higher in the case of PAC nanocomposite as compared to neat PANI. Reduction in ΔH (heat of reaction) indicates that the added nano $CaCO_3$ in PANI reduces exothermicity of polymer matrix. The $CaCO_3$ particles are absorbing the heat of reaction of polymer; hence the overall crystallinity of nanocomposite increases. The depressed peak of XRD (Fig. 1C and D) also confirm the crystalline nature of PAC nanocomposite. It is also found that the functionalized $CaCO_3$ also assists in local nucleation process; hence the crystalline nature of the composite is enhanced as compared to neat PANI. The transmission electron microscopic image (TEM) for MA coated $CaCO_3$ is shown in Fig. 3a and Fig. 3b and 3c represent the typical TEM images of PANI nanoparticles. The PANI particles appear in the range of 51–100 nm. Fig. 3d shows the TEM image of PAC nanocomposite of a sample with 4 wt.% of $CaCO_3$.

Table 2
Represent the summary for the performance of coated panels in 5% HCl, 5% NaOH and 5% NaCl.

Sr. No.	Coating system	Type of failure		
		5% HCl (for 200 h)	5% NaOH (for 200 h)	5% NaCl (for 200 h)
1	Alkyd	4, 5	2, 5	4, 6
2	1.0%PANI/alkyd	3, 4	2, 5	5, 6
3	1.5%PANI/alkyd	3	2, 5	4, 5, 6
4	2.0%PANI/alkyd	5	2	4, 6
5	2.5%PANI/alkyd	3, 4	2	4, 6
6	5.0%PANI/alkyd	4	2	6
7	1.0% PAC/alkyd	4	2	4, 6
8	1.5% PAC/alkyd	4	2	4, 5, 6
9	2.0% PAC/alkyd	3, 4	2	6
10	2.5% PAC/alkyd	4, 5	2	6
11	5.0% PAC/alkyd	4	2	6

No effect = 1; whitening = 2; shrinkage of film = 3; blistering of film = 4; Removal of film = 5; Colour change = 6.

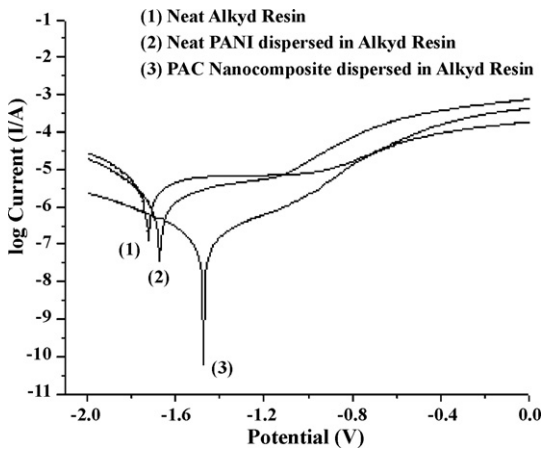

Fig. 6. Tafel plots of (1) alkyd resin, (2) PANI dispersed in alkyd resin and (3) PAC nanocomposite dispersed in alkyd resin coatings recorded in 5% NaCl solution.

The observed crystalline nature of PAC nanocomposite is confirmed by XRD gram. Some embedded black dots ($CaCO_3$ particles) having diameter 10–20 nm are also observed (Fig. 3d), which indicate that most of the $CaCO_3$ particles are finely dispersed in the PANI matrix. During initial stage of polymerization, due to hydrophobic nature $CaCO_3$, it remains with aniline (monomer/organic phase). Further, micro-mixing generated by ultrasound generates fine $CaCO_3$ embedded emulsion droplets, which leads to form finely dispersed PAC nanocomposite. A typical energy dispersive X-ray (EDX) analysis confirms the dark regions in the polymer are $CaCO_3$ nanoparticles (Fig. 3d). From all the TEM images, it is observed that the both polymer as well as $CaCO_3$ nanoparticles is in the range of nanometer and MA coated $CaCO_3$ is well dispersed in the matrix. In case of MA coated $CaCO_3$, surfactant chains (myristic acid) are adsorbed on $CaCO_3$ particle due to physical adsorption, which is a result of van der Waals forces and dipole interaction [30,35]. To confirm hydrophobicity of MA coated $CaCO_3$, it was dispersed in the mixture of organic phase and water. It is observed MA coated $CaCO_3$ remains with organic phase, while pure $CaCO_3$ found in aqueous phase.

3.2. Investigation of mechanical properties of PANI and PAC reinforced alkyd coatings

The mechanical properties of PANI/alkyd and PAC/alkyd coatings are presented in Table 1. The adhesion strength of alkyd coating is found to be an important factor in determining the coating performance to control the corrosion. Cross-cut adhesion testing (ASTM D 3359-87) during the coating process, determines the strength of the bond between substrate and coating. The coating is cut into small squares, which results in reduction of lateral bonding. The cross-cut adhesion (1 mm) of pure alkyd resin shows loss of adhesion, where as 1.0% PANI/alkyd shows marginal improvement in adhesion. The cross-cut adhesion increases as the loading of PANI increased from 1% to 5%. This is due to the enhanced adhesion between the PANI/alkyd coatings with MS plate. For aniline, the amino group and the aromatic ring are in the same plane. This coplanar orientation with respect to the metallic surface renders PANI a greater capacity to form more homogeneous films, which, in turn, translates into a better adhesion to the metal substrate.

Furthermore, the presence of a lone pair of electrons in polyaniline structure enhances the electrostatic interaction between the coatings and the metal substrate, resulting in superior cross-cut adhesion [29]. The cross-cut adhesions of PAC/alkyd were found to be higher than the PANI/alkyd coatings (Table 1). The cross-cut adhesion at identical loading was found different because of the variation in the morphology of the PANI/alkyd and PAC/alkyd coatings. The presence of MA coated $CaCO_3$ in PAC nanocomposite promotes the adhesive property as well as toughness of the coatings. Impact strength of samples are reported in Table 1, the impact strength of pure alkyd is found to be 60 kg/cm^2 and it is

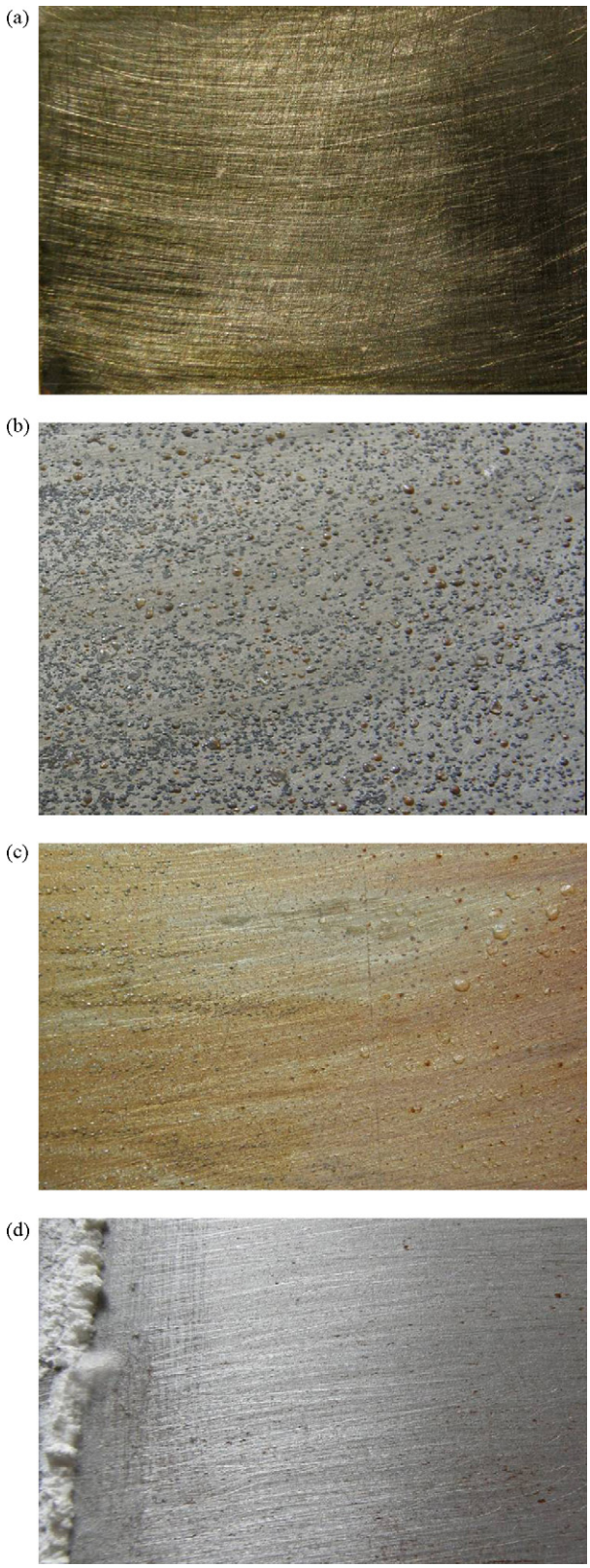

Fig. 7. PAC/alkyd coating on MS panel (a) before corrosion test; (b) in 5% HCl solution; (c) in 5% NaCl solution; (d) in 5% NaOH solution.

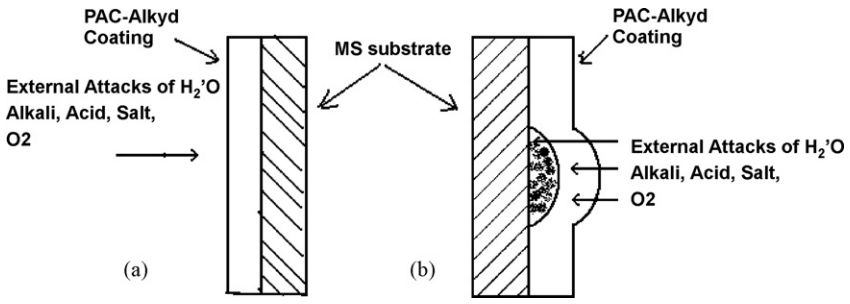

Fig. 8. Degradation mechanism in PAC/alkyd coatings. (a) initial state of surface with acid, alkali and salt access; (b) corrosion products obtained on MS plate surface.

increased to 70 kg/cm^2 by addition of 1% PANI in alkyd resin. The maximum impact strength is found to be 78 kg/cm^2 at 5% PANI loading in alkyd resin. A drastic improvement is observed when 4% of nano $CaCO_3$ is added along with varying percentage of PANI (92–102 kg/cm^2, Table 1). The improvement of impact strength from 92 to 102 Kg/cm^2 indicates that 4% $CaCO_3$ also contributes to impact strength of alkyd resin. This kind of behavior of enhancement in impact strength is because both polymer matrix and $CaCO_3$ particles are in nano-size, which impart positive effect on the alkyd coating.

It can seen from Fig. 4 that gloss values attain optimum and then decreases with the increase in % loading of PANI and PAC nanocomposite in alkyd resin. As compared to neat alkyd resin, the gloss values are found to increase with % loading of PANI and PAC nanocomposite in alkyd resin. It can be concluded that the physico-mechanical properties of the PANI/alkyd coatings are found to be significantly enhanced with the loading of the PAC nanocomposite in alkyd.

3.3. Effect of addition of PAC nanocomposite and PANI on the corrosion rate of alkyd coating

The corrosion rates (*Vc*) of alkyd resin, PANI/alkyd and PAC/alkyd were monitored for a period of 200 h. Rate of corrosion is reported in Fig. 5, while visual observations are reported in Table 2 and Fig. 7. Pure alkyd coatings disappear when placed in different corrosive media i.e. NaOH, HCl and NaCl, exhibiting a rapid corrosion rate of the pure alkyd organic coating. Corrosion rate for 0% loading of PANI or PAC nanocomposites is 0.87 cm/yr, 0.76 cm/yr and 1.024 cm/yr in case of 5% HCl solution, 5% NaCl solution and 5% NaOH solution respectively. Corrosion rate of alkyd coating is found to decrease by increase in the addition of PANI and PAC nanocomposite in alkyd resin. For 1% loading of PANI, the rate of corrosion is of the order of 0.7 cm/yr and reduces to 0.35 cm/yr units, when 5% PANI loaded in alkyd resin. With 1% PAC nanocomposite loading, the rate of corrosion is 0.42 cm/yr and it reduces to 0.1 cm/yr, when the PAC nanocomposite loading is maintained at constant value of 5% in alkyd resin in HCl solution. The value of corrosion rate is found to be very close for 5% PAC nanocomposite and PANI when alkyd coating is dipped into NaOH and NaCl solutions (0.25 and 0.21 cm/yr for PANI and PAC nanocomposite in NaOH and close to 0.1 for NaCl solution). When the loading is 5% in alkyd resin, both PANI and PAC nanocomposite showed the best performance in the case of NaCl solution. It can be concluded that 5% loading of PAC in alkyd resin is more effective for decreasing rate of corrosion in acid, alkali and salt solutions. From the corrosion rate data, it can be inferred that PANI can be replaced with PAC nanocomposite. Phenomena like removal of film, and colour change observed for alkyd coatings are minimized with increase in % of PANI loading. It is observed that above 1.5% of PAC/PANI laoding removal of film was not observed. It means that the loading of PAC or neat PANI can improve the adhesion onto the metal substrate. This clearly indicates the improvement in degradation resistance of the coating. This is also observed by Alam et al. [31,32].

In the case of PANI/alkyd, a compact iron/dopant complex layer formation at the metal-coating interface acts as a passive protective layer. PANI has redox capability to undergo a continuous charge transfer reaction at the metal-coating interface, in which PANI is reduced from emeraldine salt form (ES) to an emeraldine base (EB) [36]. On accumulation of excessive corrosive ions, alkalization of coating takes place, followed by a breakdown of the passive layer. This type of corrosion protection usually depends on the strength of the passive oxide film. The protective behavior depends on the size and charge of the dopant i.e., as the size of the dopant increases, the strength of the iron/dopant complex film increases, which improves the protective efficiency [36–38]. Laco and co-workers [39] have also reported the same kind of visual observations of growth of resultant bubble that leads to fracture and disappearance of coating (Fig. 7). However, the corrosion rate of PAC/alkyd was found to decrease appreciably with increase in the PAC nanocomposite loading in alkyd (Fig. 5a–c). In the case of PAC/alkyd, the inhibition effect of the nanocomposite coatings can be attributed to the presence of $CaCO_3$ particles. And also the small pore size and uniform dispersion of the PAC nanocomposite in alkyd helps in the formation of a well-adhered, dense, and continuous network-like structure, that slows down the penetration of the corrosive ions through the metal substrate, and inhibits the MS from the attack of the corrosive species [40]. Hence, the PAC/alkyd coatings act as excellent inhibitor to protect metals from corrosion.

Fig. 6 shows the Tafel plot for neat alkyd resin, PANI-alkyd and PAC nanocomposite-alkyd coating. I_{corr} and E_{corr} values were calculated from intersection of coordinates of Tafel plot. It is found that electrochemical current was decreased from 0.89 to 0.03 μA/cm^2, when neat alkyd resin and PAC nanocomposite was tested in NaCl electrolyte solution. Observed corrosion current for neat alkyd coating was 0.89 μA/cm^2, while for PANI-alkyd and PAC nanocomposite-alkyd coating shows 0.50 and 0.03 μA/cm^2 respectively. Additionally, E_{corr} value shows shifts in positive side from −1.74 to −1.47 V by addition of PAC composite into alkyd coating. Overall results indicates that PAC nanocomposite shows improvement in anticorrosive properties which supports the earlier corrosion rate data obtained by dip test method (Fig. 5).

3.4. Corrosion mechanism of PANI/alkyd and PAC/alkyd coatings

The corrosion mechanism in the case of PANI/alkyd and PAC/alkyd coatings is illustrated in Fig. 8. The adhesion of coating could be important factor which control the corrosion rate. PANI/alkyd and PAC/alkyd coating undergo surface crazing phenomenon due to the diffusion of oxygen, acidic, and alkaline ions (Fig. 8b). Due to attack of acid, salt, and alkali metal iron complexes (Fe^{2+}, etc) are formed. Due to alkyd cross-linking and hydrogen bonding of alkyd with PAC nanocomposite, coating becomes more compact [41,42]. Compact cross-linking of alkyd resin and

hydrophobic nature of $CaCO_3$ inhibits the moisture infiltration and moisture contact with metal through barrier mechanism, which is inferior in case of neat alkyd coatings. While PANI has ability to sore some charges (Fe^{2+} etc) generated by corrosion on mild steel panel (passivation of metal). It is reported that small quantity of PANI acts as electrochemical inhibitor and electrochemical properties of PANI nanocomposite film provides additional backup for protection. Both electrochemical and barrier mechanism communally gives the corrosion protection to mild steel [21,27].

4. Conclusion

PAC nanocomposite has higher capacity to form more homogeneous films. When PAC composite is added to alkyd resin, it leads to a better adhesion to the metal substrate. The cross-cut adhesion increases as the loading of PANI increased from 1% to 5%. This is due to the enhanced adhesion between the PANI/alkyd coatings with MS plate. Due to addition of 4% $CaCO_3$ in PANI matrix, there is a gain in impact strength of PAC/alkyd coatings. The enhancement in impact strength is because of presence of nano-size polymer matrix and $CaCO_3$. The corrosion rate of PAC/alkyd was found to decrease appreciably with the increase in the PAC nanocomposite loading in alkyd resin. It can be concluded that 5% PAC nanocomposite loading is effective for decreasing corrosion rate of alkyd resin along with improvization in mechanical properties.

Acknowledgments

S.H. Sonawane acknowledges the Department of Science and Technology (Govt. of India) for providing the funding under the grant number SR/FTP/ETA-35/2007. Authors are also thankful to Vishwakarma Institute of Technology, Pune for providing the facility for this work. Authors are also thankful to Dr M.G.Parande, A. Hage, M. Deshpande (Vishwakarma Institute, Pune), Mr Dhanaraj Shinde, (National Chemical Laboratory) for their assistance in experimental analysis.

References

[1] D.R. Baer, P.E. Burrows, A.A. El-Azab, Enhancing coating functionality using nanoscience and nanotechnology, Prog. Org. Coat. 47 (2003) 342–355.
[2] R.H. Cayton, T. Sawitowski, The impact of nanomaterials on coating technologies, NSTI-Nanotechnol. 2 (2005) 83–85.
[3] S. Zhou, L. Wu, J. Sun, W. Shen, The change of the properties of acrylic-based polyurethane via addition of nano-silica, Prog. Org. Coat. 45 (2002) 33–42.
[4] P.A. Lewis (Ed.), Pigment Handbook, vol. 1, Wiley Interscience, New York, 1988.
[5] R. Fernando, Nanomaterial technology applications in coatings, JCT Coat. Technol. 1 (2004) 32–38.
[6] N.S. Allen, M. Edge, A. Ortega, G. Sandoval, C.M. Liauw, J. Verran, J. Stratton, R.B. McIntyre, Degradation and stabilization of polymers and coatings: nano vs. pigmentary titania particles, Polym. Degrad. Stab. 85 (2004) 927–946.
[7] L.H. Yang, F.C. Liu, E.H. Han, Effects of P/B on the properties of anticorrosive coatings with different particle size, Prog. Org. Coat. 53 (2005) 91–98.
[8] L.J. Brickweg, B.R. Floryancic, E.D. Sapper, R.H. Fernando, Shear-induced 1-D alignment of alumina nanoparticles in coatings, J. Coat. Technol. Res. 4 (2007) 107–110.
[9] Q. Wang, M. Yang, Y. Chen, Effect of nano-sized iron oxide with different morphology on nanomechanical properties of nanocomposite coatings, Key Eng. Mater. 336–338 (2007) 2218–2220.
[10] L. Xue, L. Xu, Q. Li, Effect of nano Al pigments on the anticorrosive performance of waterborne epoxy coatings, J. Mater. Sci. Technol. 23 (2007) 563–567.
[11] X. Zhang, F. Wang, Y. Du, Effect of nano-sized titanium powder addition on corrosion performance of epoxy coatings, Surf. Coat. Technol. 201 (2007) 7241–7245.
[12] S. Jaroslav, T. Miroslava, B. Jitka, K. Petr, F.V. Svetlana, P. Jan, Z. Josef, Coating of zinc ferrite particles with a conducting polymer Polyaniline, J. Colloid Interface Sci. 298 (2006) 87–93.
[13] J. Jiang, L. Chao Li, F. Xu, Preparation, characterization and magnetic properties of PANI/La substituted LiNi ferrite nanocomposites, Chin. J. Chem. 24 (2006) 1804–1809.
[14] S. Mishra, S.H. Sonawane, Studies on characterization of nano $CaCO_3$ prepared by in situ deposition technique and its application in PP nanocomposites, J. Polym. Sci., Part B: Polym. Phys. 43 (2005) 107–113.
[15] A. Pud, N. Ogurtsov, A. Korzhenko, G. Shapoval, Some aspects of preparation methods and properties of polyaniline blends and composites with organic polymers, Prog. Polym. Sci. 28 (2003) 1701–1753.
[16] J.G. Gonzalez-Rodriguez, M.A. Lucio-Garcia, M.E. Nicho, R. Cruz-Silva, M. Casales, E. Valenzuela, Improvement on the corrosion protection of conductive polymers in pemfc environment by adhesives, J. Power Sources 186 (2007) 184–190.
[17] C. Jeyaprabha, S. Sathiyanarayanan, G. Venkatachari, Effect of cerium ions on corrosion inhibition of PANI for iron in 0.5 M H_2SO_4, Appl. Surf. Sci. 253 (2006) 432–438.
[18] L. Zhong, H. Zhu, J. Hu, S. Xiao, F. Gan, A passivation mechanism of doped polyaninle on 410 stainless steel in deaerated H_2SO_4 solution, Electrochim. Acta 51 (2006) 5494–5501.
[19] K.C. Chang, G.W. Jang, C.W. Peng, C.Y. Lin, J.C. Shieh, J.M. Yeh, J.C. Yang, W.T. Li, Comparatively electrochemical studies at different operational temperatures for the effect of nanoclay platelets on the anticorrosion efficiency of DBSA-doped polyaniline/Na + -MMT clay nanocomposite coatings, Electrochim. Acta 52 (2007) 5191–5200.
[20] A. Mirmohseni, A. Oladegaragoze, Anticorrosive properties of polyaniline coating on iron, Synth. Met. 114 (2000) 105–108.
[21] C. Dispenza, C. Lo Presti, C. Belfiore, G. Spadaro, S. Piazza, Electrically conductive hydrogel composites made of polyaniline nanoparticles and poly(*N*-vinyl-2-pyrrolidone), Polym 47 (2006) 961–971.
[22] Y.M. Abu, K. Aoki, Corrosion protection by polyaniline-coated latex microspheres, J. Electroanal. Chem. 583 (2005) 133–139.
[23] Z.A. Hu, X.L. Shang, Y.Y. Yang, C. Kong, H.Y. Wu, The electrochemical synthesis of polyaniline/polysulfone composite films and electrocatalytic activity for ascorbic acid oxidation, Electrochim. Acta 51 (2006) 3351–3355.
[24] W. Pan, S.L. Yang, G. Li, J.M. Jiang, Electrical and structural analysis of conductive polyaniline/polyacrylonitrile composites, Eur. Polym. J. 41 (2005) 2127–2133.
[25] A. Pud, N. Ogurtsov, N. Korzhenko, G. Shapoval, Some aspects of preparation methods and properties of polyaniline blends and composites with organic polymers, Prog. Polym. Sci. 28 (2003) 1701–1753.
[26] A.B. Samui, A.S. Patankar, J. Rangarajan, P.C. Deb, Study of polyaniline containing paint for corrosion prevention, Prog. Org. Coat. 47 (2003) 1–7.
[27] H. Zhu, L. Zhong, S. Xiao, F. Gan, Accelerating effect and mechanism of passivation of polyaniline on ferrous metals, Electrochim. Acta 49 (2004) 5161–5166.
[28] A.L.N. Silva, M.C.G. Rocha, M.A.R. Moraes, C.A.R. Valente, F.M.B. Coutinho, Mechanical and rheological properties of composites based on polyolefin and mineral additives, Polym. Test. 21 (2002) 57–60.
[29] S.H. Sonawane, S.R. Shirsath, P.K. Khanna, S. Pawar, C.M. Mahajan, V. Paithankar, V. Shinde, C.V. Kapadnis, An innovative method for effective micro-mixing of CO_2 gas during synthesis of nano-calcite crystal using sonochemical carbonization, Chem. Eng. J. 143 (2008) 308–313.
[30] S.H. Sonawane, P.K. Khanna, S. Meshram, C. Mahajan, M.P. Deosarkar, S. Gumfekar, Combined effect of surfactant and ultrasound on nano calcium carbonate synthesized by crystallization process, Int. J. Chem. Reactor Eng. 7 (2009) A47.
[31] J. Alam, U. Riaz, S.M. Ashraf, S. Ahmad, Corrosion-protective performance of nano polyaniline/ferrite dispersed alkyd coatings, J. Coat. Technol. Res. 5 (2008) 123–128.
[32] J. Alam, U. Riaz, S. Ahmad, High performance corrosion resistant polyaniline/alkyd ecofriendly coating, Curr. Appl. Phys. 9 (2009) 80–86.
[33] M. Çelik, M. Onal, Intercalated polyaniline/Na-montmorillonite nanocomposites via oxidative polymerization, J. Polym. Res. 14 (2007) 313–317.
[34] J. Jiang, L. Hong ai, Microemulsion-mediated in-situ synthesis and magnetic characterization of polyaniline/$Zn_{0.5}Cu_{0.5}Fe_2O_4$ nanocomposite, Appl. Phys. A: Mater. Sci. Eng. 2 (2008) 341–344.
[35] G. Nakai, T. Fukuda and K. Hosoi, Surface-coated calcium carbonate particles, method for manufacturing same, and adhesive, U. S. Patent 6,686,044, February 3, 2004.
[36] E. Jose, S. Pereira, I. Susana, T. Cordoba, M.T. Roberto, Polyaniline acrylic coatings for corrosion inhibition: the role played by counter-ions, Corros. Sci. 47 (2005) 811–822.
[37] V.A. Rosa, R.B. Hugo, A. Eduardo, Synthesis and characterization of polyaniline and poly-ortho-methoxyaniline. Behaviour against carbon steel corrosion, J. Chil. Chem. Soc. 48 (2003).
[38] D.C. Trivedi, Influence of the anion on polyaniline, J. Solid State Electrochem. 2 (1998) 85–87.
[39] J. Ignacio, I. Laco, F.C. Villota, F.L. Mestres, Corrosion protection of carbon steel with thermoplastic coatings and alkyd resins containing polyaniline as conductive polymer, Prog. Org. Coat. 52 (2005) 151–160.
[40] P. Zarras, N. Anderson, C. Webber, D.J. Irvin, A. Guenthner, J.D. Stengersmith, Progress in using conductive polymers as corrosion-inhibiting coatings, Radiat. Phys. Chem. 68 (2003) 387–394.
[41] N. Chisholm, H. Mahfuz, V.K. Rangari, A. Ashfaq, S. Jeelani, Fabrication and mechanical characterization of carbon/SiC-epoxy nanocompositesm, Compos. Struct. 67 (2005) 115–124.
[42] H.J. Yu, L. Wang, Q. Shi, G.H. Jiang, Z.R. Zhao, X.C. Dong, Study on nano $CaCO_3$ modified epoxy powder coatings, Prog. Org. Coat. 55 (2006) 296–300.